European Journal of Materials

ISSN: 2688-9277 (Online) Journal homepage: www.tandfonline.com/journals/tems20

Generative Adversarial Networks (GANs)-based timeseries data augmentation to overcome data scarcity in the context of material testing

Sanghyun Yoo , Amal Viswakumar , Mathieu Vinot , Nathalie Toso & Heinz Voggenreiter

To cite this article: Sanghyun Yoo , Amal Viswakumar , Mathieu Vinot , Nathalie Toso & Heinz Voggenreiter (2026) Generative Adversarial Networks (GANs)-based timeseries data augmentation to overcome data scarcity in the context of material testing, European Journal of Materials, 6:1, 2685400, DOI: 10.1080/26889277.2026.2685400

To link to this article: https://doi.org/10.1080/26889277.2026.2685400

Published online: 14 Jun 2026.

EUROPEAN JOURNAL OF MATERIALS
2026, VOL. 6, NO. 1, 2685400
https://doi.org/10.1080/26889277.2026.2685400

Taylor & Francis
by informa

CHARACTERIZATION AND MODELLING

OPEN ACCESS

Check for updates

Generative Adversarial Networks (GANs)-based timeseries data augmentation to overcome data scarcity in the context of material testing

Sanghyun Yoo[a,b], Amal Viswakumar[a,b], Mathieu Vinot[a], Nathalie Toso[a] and Heinz Voggenreiter[a]

[a]Institute of Structures and Design, German Aerospace Center (DLR), Stuttgart, Germany; [b]Innovation Center for Small Aircraft Technologies (INK), German Aerospace Center (DLR), Würselen, Germany

ABSTRACT

Data scarcity is one of the major challenges in applying machine learning, as acquiring training data on the material behaviour is often difficult due to high costs and time constraints. To address this challenge, this study reports the development of a robust data augmentation method based on Generative Adversarial Networks (GANs). Firstly, the hyperparameters of the GANs model are optimized using Bayesian Optimization by minimizing the Fréchet inception distance. Secondly, the quality of the generated data and its similarity to experimental datasets are evaluated using A-basis material allowables to determine the acceptability of the synthetic data. The accepted data are subsequently used to train a Gaussian Process Regression (GPR) model for predicting the strain-rate effect. Results show that the GPR model trained on a dataset of 1800 data points achieved a lower negative log predictive density score than the model trained only on the experimental dataset. Furthermore, a hybrid approach is introduced to integrate the GPR model with a Cowper-Symonds model, thereby further improving prediction accuracy. Ultimately, this framework establishes a robust, statistically validated method for synthetic data generation and for overcoming data limitations in the accurate modelling of the strain-rate dependent properties of carbon/epoxy composites.

ARTICLE HIGHLIGHTS

- A Generative Adversarial Networks (GANs) framework is developed to address data scarcity in the context of material testing.
- This framework significantly reduces the cost and time of physical testing by generating statistically validated synthetic data.
- Gaussian Process Regression (GPR) is integrated with the Cowper-Symonds model to improve the predictive accuracy of strain-rate effect on the in-plane shear strength of carbon/epoxy composites.

ARTICLE HISTORY
Received 30 December 2025
Revised 2 April 2026
Accepted 1 June 2026

KEYWORDS
Mechanical properties prediction; machine learning; data augmentation; Generative Adversarial Networks (GANs); Gaussian Process Regression (GPR)

1. Introduction

Machine learning (ML) models have recently gained popularity in the prediction of material properties and material design parameters (Dev et al., 2024; Dornheim et al., 2024; Furtado et al., 2021; Ge et al., 2025; Kibrete et al., 2023; M. Liu et al., 2024; X. Liu et al., 2021; Malashin et al., 2025; Shah et al., 2022; Sorour et al., 2024). Several review papers (Kibrete et al., 2023; X. Liu et al., 2021; Sorour et al., 2024) have surveyed the integration of ML models for predicting the mechanical properties of composite materials. A common finding in these studies is that although the ML models demonstrate considerable capabilities, their application and reliability are often hindered by the lack of sufficient and high-quality training data (*i.e., data scarcity*). Having a large amount of data is essential for training ML models as it helps them learn patterns and accurately predict target values (Alzubaidi et al., 2023; Hakami, 2024). Data scarcity presents considerable challenges in training these models as it could lead to overfitting and poor generalization (Alzubaidi et al., 2023; Bansal et al., 2022). To address this data scarcity, researchers have prepared training data from several sources, such as

CONTACT Sanghyun Yoo sanghyun.yoo@dlr.de Institute of Structures and Design, German Aerospace Center (DLR), Stuttgart, Germany.

compiling values from published literature (Huang et al., 2021; Su et al., 2024), integrating physical models (Pandya et al., 2020), conducting extensive experiments (Karamov et al., 2022; Q. Liu & Wu, 2024), or using finite element (FE) simulations (Freed et al., 2022; X. Liu et al., 2023; Reiner et al., 2021; Sakaridis et al., 2022; Zhang et al., 2022).

For example, a common approach to generate large virtual datasets is using FE simulations. Reiner et al. (2021) introduced a framework that uses ML and FE modelling to characterize the strain-softening behaviour of carbon fibre-reinforced polymers (CFRP) composites under compressive loads. They used the continuum damage Mechanics (CDM) based FE simulations to simulate compact compression tests of quasi-isotropic IM7/8552 CFRP and create a large virtual dataset. The study found that the Long Short-Term Memory (LSTM) model, when trained with at least 5000 FE simulations, accurately predicted the material's response. The trained LSTM model was then successfully validated against experimental data from a variety of compressive tests. However, a large number of simulations are required to predict material properties with simulation-based approaches, resulting in a high computational cost. Thus, data-driven solutions are needed to further accelerate data generation process.

Data augmentation is a technique used to enhance the dataset by generating new data from the existing real data and offers a promising solution to tackle data scarcity (Bansal et al., 2022). Common augmentation techniques include random transformations such as rotation, scaling, and noise addition and are widely used in training ML models for image processing. However, random transformation-based data augmentation methods are not suitable for timeseries data because it could distort the temporal dependencies and underlying sequential patterns (Annaki et al., 2024; Iglesias et al., 2023; Iwana & Uchida, 2021; Wen et al., 2021). An effective alternative for timeseries data is to use generative ML models to generate new data points based on the original data. Generative models like Generative Adversarial Networks (GANs) and Variational Autoencoders (VAEs) can learn the underlying data distribution and temporal dependencies of the original dataset (Goodfellow et al., 2014; Ho et al., 2020; Kingma & Welling, 2019; Luleci & Catbas, 2023). By generating new data, this approach adds significant informational value to the dataset and enables the creation of a large volume of data.

The application of data augmentation techniques based on generative models is established for tabular material data (Qu et al., 2025; Zhou et al., 2025) and in several domains relying on timeseries data (Demir et al., 2021; L.-M. Liu et al., 2023; H. Yang et al., 2025). For example, H. Yang et al. (2025) reported the use of the GANs model in predicting the ignition process of solid rocket motors (SRMs). They demonstrated that synthetically enhanced data in conjunction with the original data led to a notable increase in the prediction accuracy. Similarly, increasing the size of input training data using the GANs model has proven effective for the case of image-based applications (Alqahtani et al., 2021; Jain et al., 2022; Melching et al., 2023). For instance, Jain et al. (2022) reported the use of the GANs to create synthetic images of surface defects. This approach addressed the challenge posed by limited annotated data for training industrial inspection algorithms. When synthetic data were used to enhance the training of a Convolutional Neural Network (CNN) for steel defect classification, a significant performance improvement was achieved with a sensitivity increasing from 90.28% to 95.33% compared to traditional augmentation methods.

Acquiring training data in material science, whether the data are derived from extensive physical testing or high-fidelity FE simulations, highlights a significant bottleneck. This data scarcity severely restricts the development of robust models and creates a clear need for efficient and data-driven approaches to synthetically augment training data. Furthermore, while various timeseries data augmentation methods are available (Chatterjee et al., 2025; Nikitin et al., 2024; Turowski et al., 2024), they are often insufficient for being directly applicable for because they do not account for the temporal dependencies inherent in material testing data. Also, these methods typically lack evaluation criteria that are tailored to the unique material properties and constraints of material data. Consequently, there is a significant need to adapt these generative strategies to handle sequential material test data like stress-strain curves.

To address this research gap, this paper presents a comprehensive data augmentation method to generate and evaluate synthetic timeseries data and aims specially at addressing the challenge of data

scarcity. A data augmentation technique based on a GANs model is developed to capture the underlying temporal relationships inherent in real experimental data. Lastly, we present a case study to demonstrate how these augmented data can be used to predict the strain-rate dependent shear properties of carbon/epoxy composites using Gaussian Process Regression (GPR).

1.1. Generative Adversarial Networks (GANs)

The GANs model is a neural network-based generative model consisting of two neural networks that are a generator (G) and a discriminator (D) (Alqahtani et al., 2021; Goodfellow et al., 2014). The role of the generator is to create convincing fake data $\hat{x}$ from a latent variable z, which is sampled from a random distribution. These generated data, along with data from the real dataset x, are then fed as input to the discriminator. The discriminator acts as a classifier to determine whether the input it receives is real or fake. As shown in Figure 1, these two networks are trained in opposition to each other. The generator attempts to produce realistic data so that the discriminator cannot distinguish it. The discriminator needs to be performing well enough to effectively distinguish real data in the output from the generator.

In the GANs model, the generator and the discriminator play a two-player zero-sum (min-max) game. The adversarial training process continues until the generator ideally produces high-quality synthetic data that are indistinguishable from real data. The game is defined by a value function $V(D,G)$, and the standard minmax objective is defined as:

$$\min_G \max_D V(D,G) = \mathbb{E}_{x\sim\mathbb{P}_r}\left[\log D(x)\right] + \mathbb{E}_{z\sim\mathbb{P}_z}\left[1-\log D\left(G(x)\right)\right] \qquad (1)$$

where z is the latent vector, which is generated randomly by a uniform or Gaussian distribution, where $z\sim\mathbb{P}_z$ and $x\sim\mathbb{P}_r$ is real distribution.

The objective function is implemented using a Binary Cross-Entropy (BCE) loss function, as the discriminator is performing a binary classification (real or fake). The discriminator is trained to correctly identify both real and fake sample. The class of real data is labelled as 1 while the class of fake data from the generator is labelled as 0. Its training objective is to maximize the probability of making a correct classification, pushing its output for real data $D(x)$ towards 1 and its output for fake data $D\left(G(z)\right)$ towards 0. On the other hands, the objective of the generator is to fool the discriminator. For this, only synthetic data are taken to train the discriminator to misclassify its fake data as real. The label for synthetic data given as input to the discriminator is taken as 1. Thus, the loss of the generator minimizes when $D\left(G(z)\right)$ is pushed towards 1. This training process reaches a convergence when the generator produces data so realistic that the discriminator is no longer able to distinguish it from real data. At this point, the discriminator is essentially guessing and its output for both real and fake data approaches $D(x)=D\left(G(z)\right) = 0.5$.

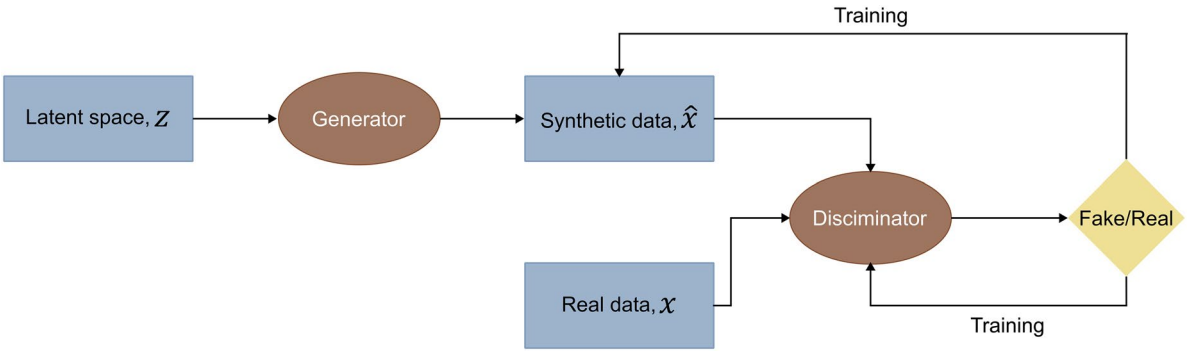

Figure 1. Flowchart of Generative Adversarial Networks (GANs) architecture Image created by the author, adapted from Alqahtani et al., 2021).

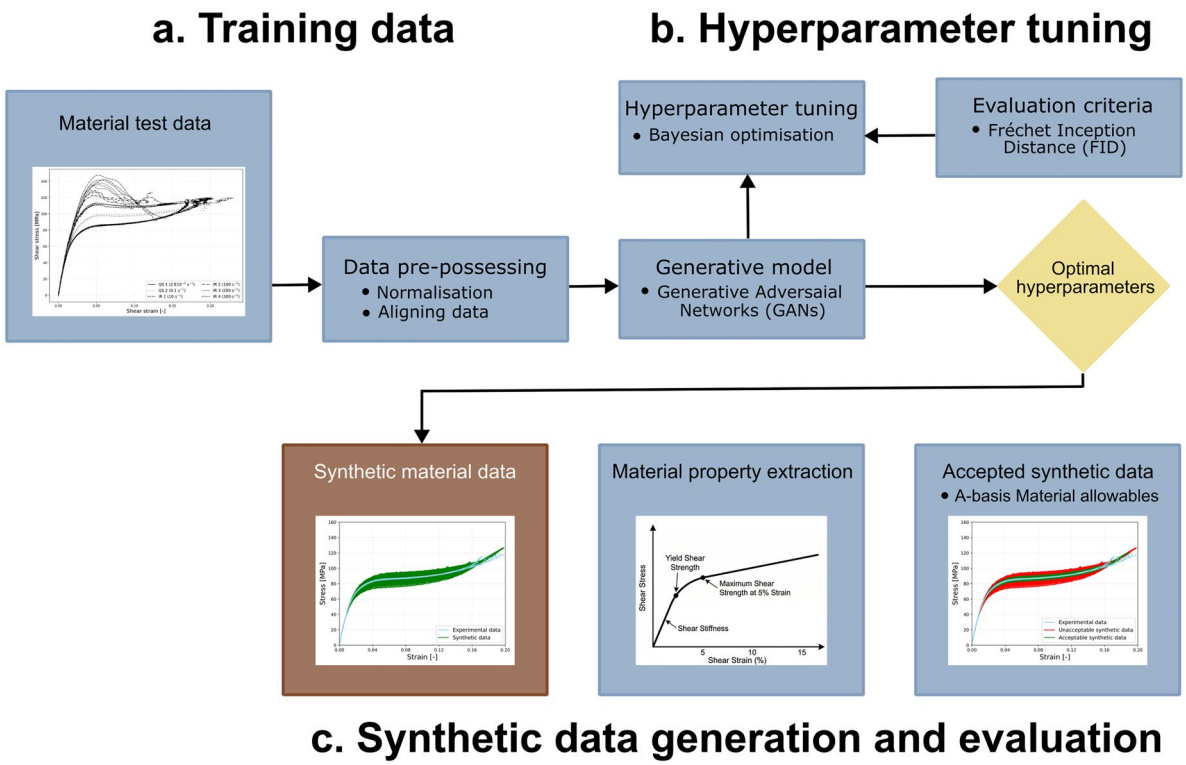

Figure 2. Overview of the workflow for GANs-based data augmentation: a. experimental input data; b. hyperparameter tuning using Bayesian optimization; c. synthetic data generation and evaluation using A-basis material allowables.

2. Modelling framework

Figure 2 illustrates the framework for a GANs-based data augmentation technique designed to create synthetic data that closely resemble real experimental data. Experimental data are pre-processed using Python libraries such as Scikit-learn and NumPy. This pre-processing step involves cleaning and scaling the input data to ensure that each variable contributes equally to the model. Meanwhile, the GANs model is modelled using Pytorch (Paszke et al., 2019). Following this, Bayesian Optimization (BO) is employed using Ray Tune (Liaw et al., 2018) for hyperparameter tuning. The synthetic data are generated using the GANs model and the resulting data are accessed by A-basis material allowables to ensure quality and to statistically validate its similarity to the input experimental data.

2.1. Training data

For the training of the GANs model, experimental data obtained from the previous study are used, and the details of experimental set-ups can be found in Yoo et al. (2022). Dynamic in-plane shear properties of IM7/8552 CFRP composite are examined up to nominal strain-rate of 300 s^{-1} to investigate the strain-rate dependent behaviour of carbon/epoxy composites. It should be noted that three to five experimental tests are conducted per each strain-rate. Therefore, the training dataset consists of the total 18 stress-strain curves with three repetitions at six different strainrates.

2.2. Hyperparameter tuning

ML models require careful selection of hyperparameters since optimal hyperparameters can directly impact the model's performance and prediction accuracy (L. Yang & Shami, 2020). This process, known as hyperparameter tuning, aims at identifying the optimal set of values by maximizing or minimizing a model's objective function. Several popular optimization methods including grid search, random search, genetic algorithms (GA) and Bayesian Optimization (BO) are employed for this purpose (Vincent & Jidesh, 2023).

In this study, BO is implemented because it can often find best hyperparameters in fewer iterations compared to random methods and can facilitate an automatic tuning process (Snoek et al., 2012; Wang et al., 2023). BO aims at modelling a probabilistic surrogate model of the objective function, which estimates the model score for a given set of hyperparameters. The process starts by evaluating the model with a few initial hyperparameter sets, which are used to build the first version of the surrogate model. Then, BO iteratively repeats an optimisation process. Mathematically, let H be the hyperparameter search space, which contains all possible hyperparameters, $h \in \mathcal{H}$ be a specific set of hyperparameters, and $f(h)$ be the expensive-to-evaluate objective function. Then, BO finds optimal hyperparameters h^* for the model, and it can be formulated as:

$$h^* = arg\max_{h \in \mathcal{H}} f(h) \qquad (2)$$

Figure 3 illustrates the overall workflow for hyperparameter tuning. Firstly, an acquisition function that guides the search is used to determine the most promising set of hyperparameters for a next evaluation. After that, the ML model is trained and evaluated with the hyperparameters from the previous step. The resulting hyperparameter and its score are used to update the surrogate model, thereby improving the accuracy for the next iteration. Finally, the surrogate model is updated with each iteration and the hyperparameters that yield the optimal objective score are selected as the best hyperparameters.

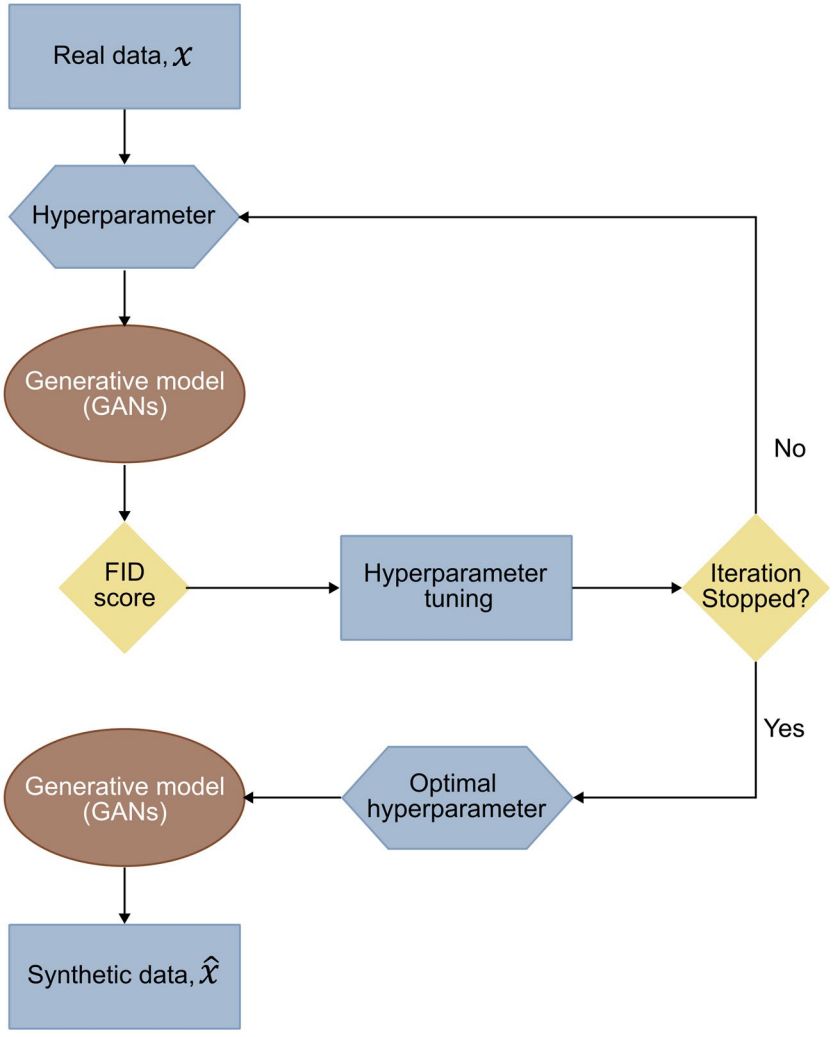

Figure 3. The flowchart of hyperparameter tuning.

2.2.1. Fréchet inception distance (FID)

Generative models are evaluated based on the quality and nature of the generated data compared to real data. Various evaluation metrics are used to quantify the similarity between these two datasets (S. Guan & Loew, 2019). Distance metrics are a prominent class of these evaluations and measure the distance between the statistical distributions of the real and of the generated datasets. A widely used and effective metric is the Fréchet inception distance (FID) score, which is measuring the Fréchet distance between these two Gaussian distributions (S. Guan & Loew, 2019; Heusel et al., 2017). A smaller distance implies that the two distributions are more similar and implies the generated data are resemble to experimental data. Thus, the FID score of 0 is ideally indicating a perfect match between the two distributions. The FID score between the real data distribution (R) and the generated data distribution (G) is given as:

$$FID(R,G) = \left\|\mu_r - \mu_g\right\|_2^2 + Tr\left(\Sigma_r + \Sigma_g - 2\left(\Sigma_r\Sigma_g\right)^{1/2}\right) \quad (3)$$

where, μ_r and μ_g are the mean vectors of the features for the real and generated data, respectively. Σ_r and Σ_g are the covariance metrices of the features for the real and generated data, respectively.

2.2.2. Optimal hyperparameters

In this study, the FID score is used as an objective function, which the optimizer sought to minimize iteratively over 1000 BO trials. The FID is directly computed on stress-strain data by calculating the statical distance between the real and synthetic datasets. Thus, it should be noted that while FID serves as a robust statistical metric to measure distributional similarity, it does not explicitly enforce constitutive material laws. Consequently, the FID is utilized solely as the objective function to ensure the baseline shape of stress-strain data generated prior to acceptable criteria (refer to Section 2.4).

This process identifies the optimal set from the hyperparameter search space detailed in Table 1. To reduce the dimensionality of the search space and enforce stability, several parameters are fixed. The GANs model architecture is constrained to three hidden layers and the ADAM optimizer with decay rates are set to β_1 = 0.25 and β_2 = 0.999. Fixing these values allowed the optimisation to focus on the remaining parameters in the search space. Following the completion of the optimisation, the best-performing set is identified. This set of hyperparameters achieved the lowest FID score of 0.42 in the search and the optimal values are presented in Table 2 along with the resultant performance.

Table 1. Hyperparameter search space.

Hyperparameters	Search space range [min, max]	Description
Neurons in hidden layers	[2, 50]	Number of neurons in the hidden layers.
Learning rate	[11E−6, 1E−2]	Learning rate for the Adam optimizer.
G/D iterations	G: [1, 5], D: [1, 5]	Ratio of generator (G) to discriminator (D) training steps per epoch.
Latent vector	[15, 25]	Dimensionality of the input noise vector (z).
Regularizer	[1E−6, 1E−2]	Coefficient for L2 weight regularization.

Note: G: generator; D: discriminator.

Table 2. Optimal hyperparameters and the summary of GANs performance.

Parameter	Optimal hyperparameters
Neurons in hidden layers	G: [40, 32, 43], D: [15, 9, 46]
Learning rate	G: 7.7E−4, D: 2.3E−3
G/D iterations	G: 2, D: 1
Latent vector	22
Regularizer	G: 5.3E−3, D: 8.9E−3
FID score	0.42
Number of weight parameters in the optimal model	≈ 290k
Total time taken for data generation with optimal parameters	≈ 39 s

Note: G: generator; D: discriminator.

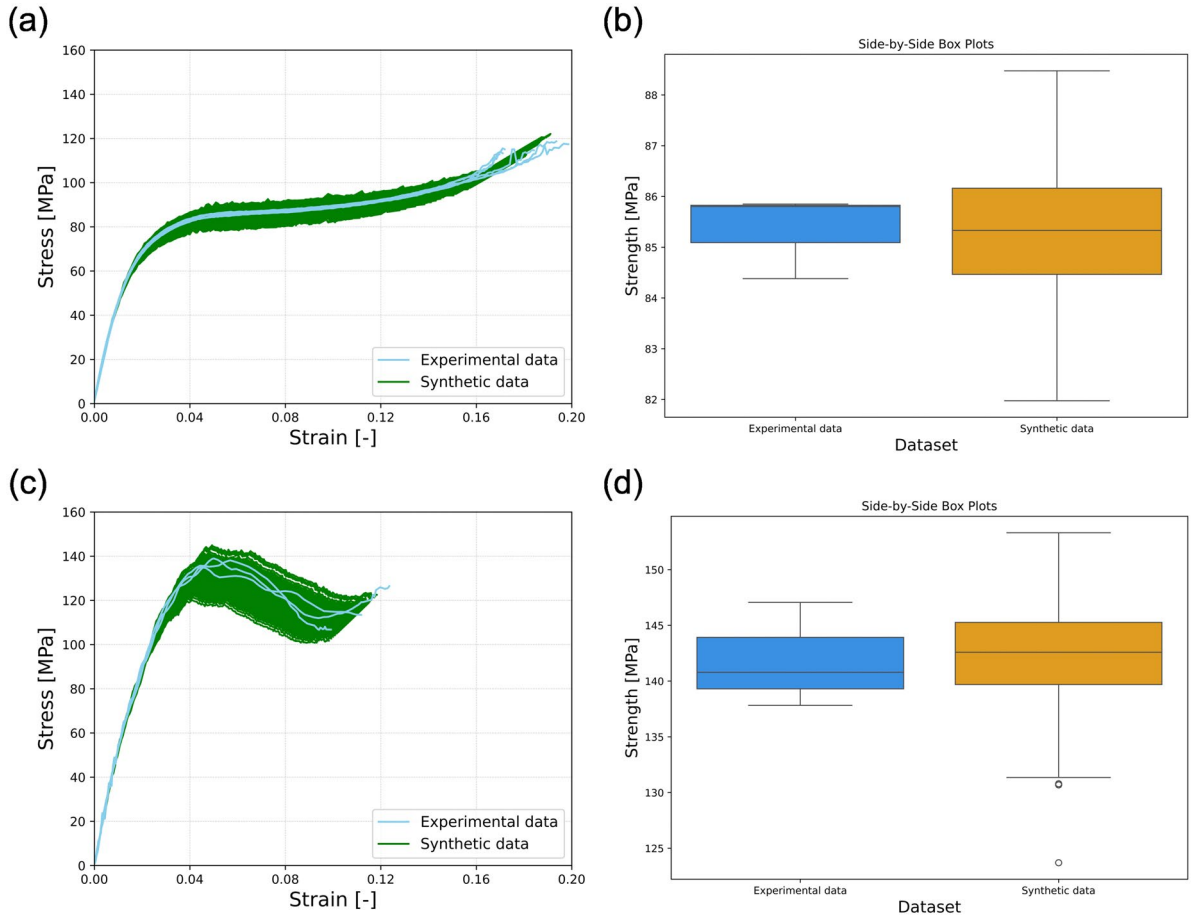

Figure 4. Comparison of synthetic data generated by the GANs model and experimental data: (a) comparative study on stress-strain data at quasi-static condition; (b) statistical strength distribution at quasi-static condition; (c) comparative study on stress-strain data at strain-rate of 300 s^{-1};(d) statistical strength distribution at strain-rate of 300 s^{-1}.

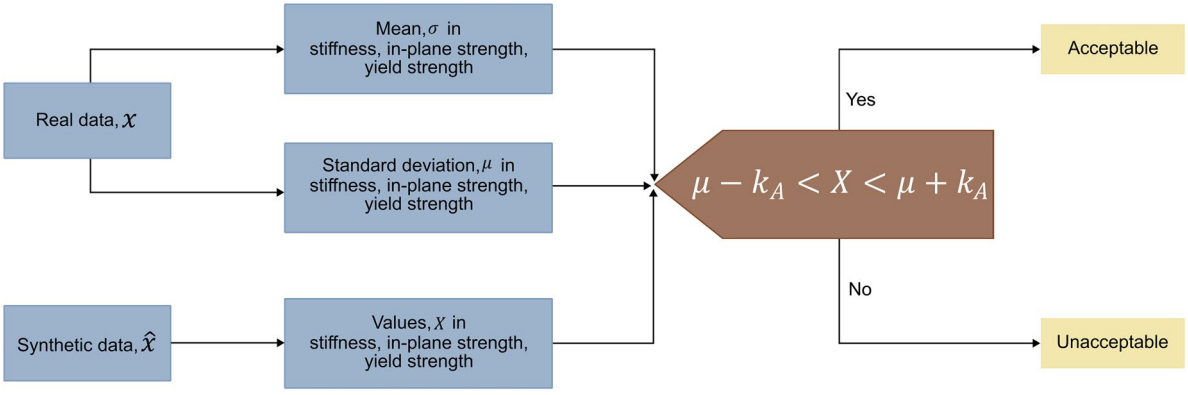

Figure 5. Flowchart for acceptance criteria using A-basis design allowables

2.3. Synthetic data generation

Figure 4 shows a comparison between the synthetic data generated by the GANs model and real experimental data. In Figure 4(a), 500 synthetic data and experimental data measured at quasi-static condition is presented. The visual comparison demonstrates that the synthetic data resemble the real data and clearly mimic the overall behaviour of the stress-strain data including elastic and plastic regions. The generated data successfully captures the material behaviours of the IM7/8552 composites as the stress-strain data precisely follow the initial elastic region, the yield point and the subsequent plastic region.

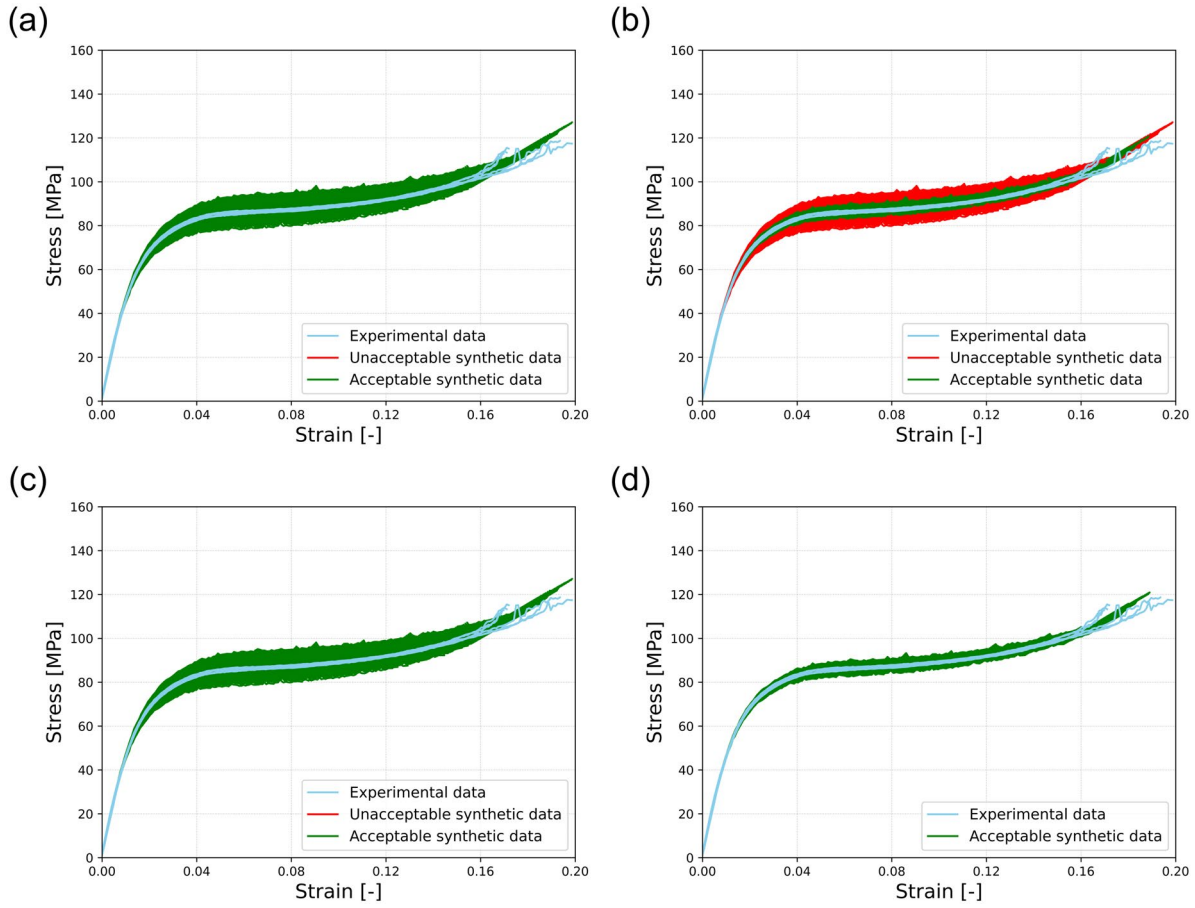

Figure 6. Application of acceptable criteria based on A-basis material design allowables: (a) shear modulus; (b) in-plane shear strength; (c) yield strength; (d) final accepted stress-strain data.

The side-by-side box plot shown in Figure 4(b) compares the quantitative distribution of the extracted in-plane strength at a strain of 5%. This plot confirms that the statistical characteristics of synthetic data align well with the real experimental data. The median, which is the line in the middle of the box, shows a good agreement with a low root mean square error (RMSE = 2.85) between the synthetic data and the experimental data and suggests that the synthetic dataset is statistically indistinguishable from the experimental dataset. While the interquartile range of the experimental data is narrow, ranging from 85 to 86 MPa, the synthetic data exhibit a much broader range of strength values. This could imply that the GANs model suggests a larger population variability that leads a larger standard deviation than experimental data. Additionally, a deviation between the experimental and the synthetic data is observed after a strain of approximately 0.18. This finding indicates that the significant scatter observed in the experimental data within this range leads to a less dense input data distribution. As a result, the GANs model, which learns from the probability distribution of the input data, may struggle to generalize effectively with this input distribution. Consequently, it might not accurately capture the variability present in the experimental data after strain of 0.18. Furthermore, a similar trend can be found between the synthetic and the experimental data at a strain-rate of 200 s^{-1} as shown in Figure 5(c,d). This observation indicates that the synthetic data generated from the GANs model is realistic and comparable to the experimental data.

2.4. Evaluation criteria

2.4.1. Material design allowables

Material allowables are statistically derived material data that are used in the design and certification of composite structures in the aerospace industry. These values are used to ensure the required level

of structural safety and the procedures are established by the Composite Material Handbook (CMH-17) (Cumbo et al., 2022; SAE International, 2012). There are two types of statistically determined allowables, A-Basis and B-Basis. For example, the A-basis material allowables indicate that at least 99% of the population of material values is expected to meet or exceed this tolerance level with 95% confidence level.

In this study, A-Basis material allowables are used to evaluate the augmented synthetic data and assess whether these values are acceptable in terms of statistics. The criteria for acceptance is established to determine if the distribution of the material properties from experimental data aligns with that of the synthetic data. The mean σ and standard deviation μ of generated data must be in the range of $\sigma \pm k_A(\mu)$ of the material properties of experimental data. The A-basis tolerance factors k_A, and the coefficients, c_A, b_A, Q are given by (Tomblin et al., 2003):

$$k_A = z_A\sqrt{\frac{f}{Q}} + \sqrt{\frac{1}{c_A n} + \left(\frac{b_A}{2c_A}\right)^2} - \frac{b_A}{2c_A} \tag{4}$$

$$b_A = 2.0643\left(\frac{1}{\sqrt{f}}\right) - 0.95145\left(\frac{1}{\sqrt{f}}\right) + 0.51251\left(\frac{1}{f\sqrt{f}}\right) \tag{5}$$

$$c_A = 0.369161 + 0.0026958\left(\frac{1}{\sqrt{f}}\right) - 0.65201\left(\frac{1}{\sqrt{f}}\right) + 0.011320\left(\frac{1}{f\sqrt{f}}\right) \tag{6}$$

$$Q = f - 2.327\sqrt{f} + 1.138 + 0.6057\left(\frac{1}{\sqrt{f}}\right) - 0.3287\left(\frac{1}{f}\right) \tag{7}$$

where f is the degrees of freedom for the variance and z_A is the standard normal random variable with a value of 2.32635 (99% probability).

After the estimation, a k_A of 4.13 is achieved with the five samples at quasi-static condition. The workflow of the acceptance criteria is given in Figure 5. The material properties considered are the stiffness, yield strength and the maximum strength at strain 5% as in-plane shear strength, and those properties are calculated in accordance with ASTM D3518/D3518M (ASTM D3518/D3518M-18, 2018). The acceptance criteria is applied to each property individually and then the intersection of all the allowable curves is taken as accepted stress-strain data.

Figure 6(a–c) shows the application of acceptance criteria to determine acceptable or unacceptable generated stress-strain data along with the real experimental data in shear modulus, in-plane shear strength at 5% strain, and yield strength, respectively. The intersection of these accepted data for each property is used to obtain the final acceptable data, as shown in Figure 6(d). The results show that in-plane shear strength is the critical material property for determining the acceptability of synthetic data, and the percentage of acceptable data under this criterion is between 85 and 95%.

2.4.2. Comparison between modelled and experimental data

Figure 7(a–c) shows the Probability Density Functions (PDF) distribution of different material properties such as shear modulus, in-plane shear strength and yield strength. The PDF shows the diversity of the synthetic data generated by the GANs model compared to experimental data. A good qualitative match between the generative model and experiments is confirmed by comparing the mean and coefficient of

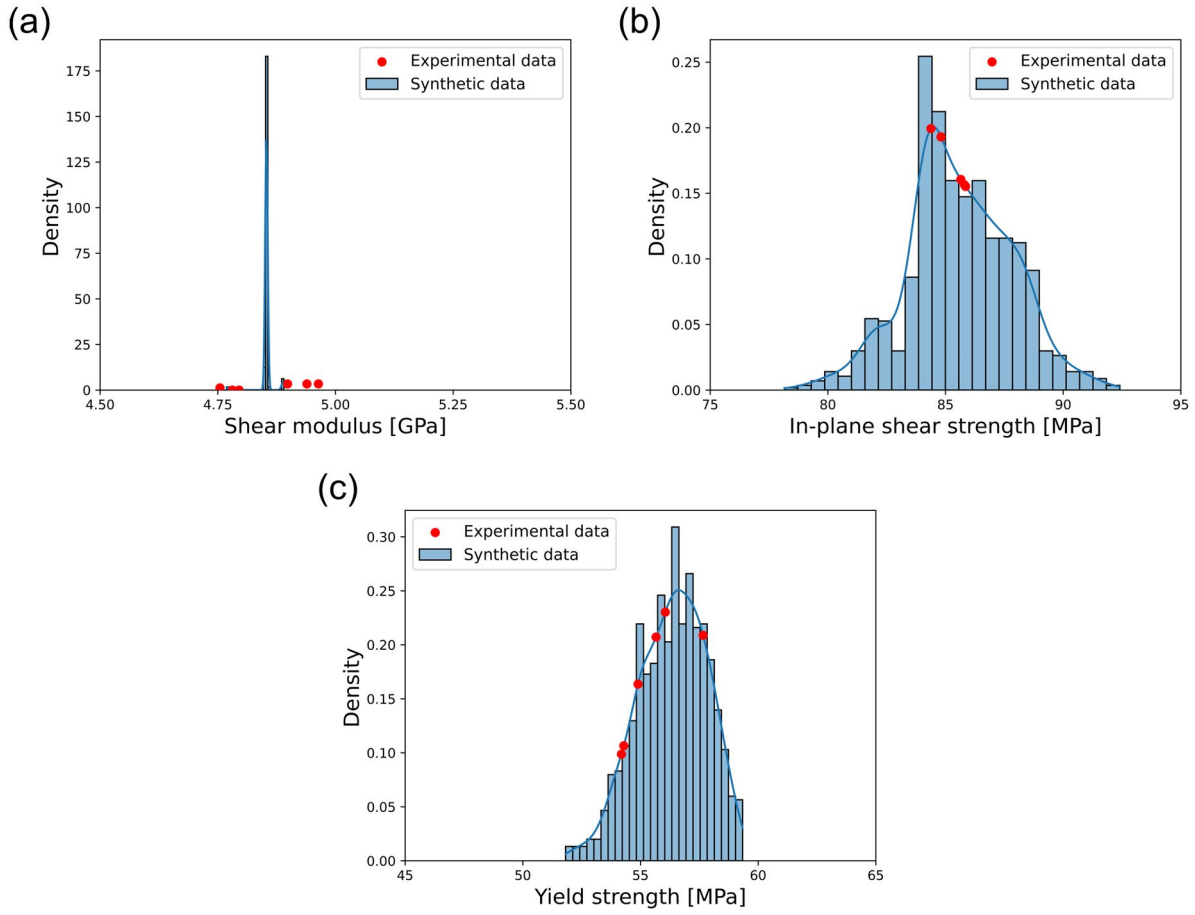

Figure 7. Probability density from generated synthetic data compared to experimental data: (a) shear modulus; (b) in-plane shear strength; (c) yield strength.

Table 3. Summary of GANs-generated and experimental mean properties and their corresponding standard deviation.

Properties	Experimental data	Synthetic data
Shear modulus [GPa]	4.86 ± 0.08	4.85 ± 0.01
In-plane shear strength at 5% strain [MPa]	85.22 ± 0.57	85.58 ± 2.23
Yield strength [MPa]	55.46 ± 1.19	56.34 ± 1.47

variation of the in-plane shear strength values. Furthermore, Table 3 presents the summary of quantitative comparison between the extracted material properties from experiments and from the synthetic data.

3. A case study on the prediction of strain-rate effects

3.1. Problem statement

Strain-rate effect in carbon/epoxy composites can be empirically examined through Cowper-Symonds (CS) model (Koerber et al., 2018; Thomson et al., 2025) and this phenomenological model incorporates two fitting parameters, K and n:

$$\mathrm{f}\left(\dot{\epsilon}\right)=1+\left(K\dot{\epsilon}\right)^{\frac{1}{n}} \qquad (8)$$

where $\dot{\epsilon}$ is strain-rate.

The CS model is an example of curve fitting, which is based on a pre-defined semi-logarithmic equation explicitly to describe the relationship between the strain-rate and the material's response.

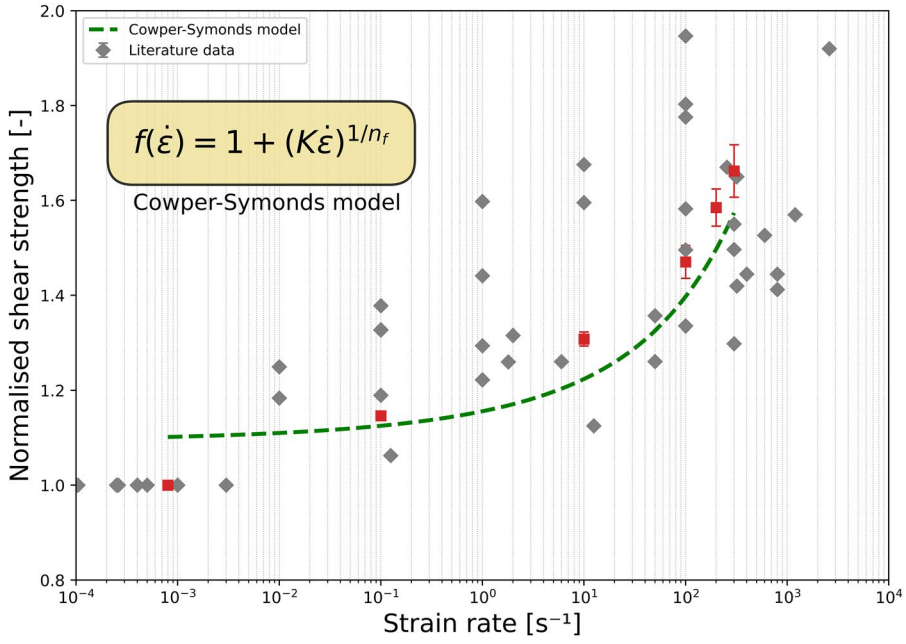

Figure 8. Comparison of in-plane shear strength with the values predicted from the current study and published experimental results (Cui et al., 2016; Daniel et al., 2018; Gilat et al., 2002; Hsiao et al., 1999; Koerber et al., 2010, 2018; Ledford et al., 2021; Lienhard & Böhme, 2015; Rouf et al., 2024; Taniguchi et al., 2007, 2008; Thomson et al., 2017).

Figure 8 illustrates the normalized experimental data to the quasi-static value, alongside published data in literature (Cui et al., 2016; Daniel et al., 2018; Gilat et al., 2002; Hsiao et al., 1999; Koerber et al., 2010, 2018; Ledford et al., 2021; Lienhard & Böhme, 2015; Rouf et al., 2024; Taniguchi et al., 2007, 2008; Thomson et al., 2017). A fitted curve with the fitting parameter of K=0.55 and n=0.25 is found when experimental data used in this study are solely considered. This results clearly reveal that the in-plane shear strength increases with increasing strain-rates and a similar trend is also reported in literature for carbon/epoxy composites (Thomson et al., 2025).

However, it can be seen that the best-fit curve does not fully converge with the experimental data, especially at lower strain-rates. Although it provides simple and computationally trivial estimations, the fitting process often requires numerical optimisation algorithms to find the optimal fitting parameters that make the best-fit to experimental data. Consequently, the selection of algorithms and parameters is inherently subjective and relies significantly on the user's experience. Furthermore, compared to literature data, the resulting parameters could become highly uncertain. This is because a small amount of experimental data is used and the literature data possess a high scatter (refer to Figure 8). The model's validity is entirely depending on the quality of input data since the fitting parameters for the model are derived from experimental data. Also, such model is deterministic, so it provides no information about the confidence of the prediction.

As quantifying uncertainty is required for reliable prediction, especially important for a safety-critical industry like aerospace and healthcare, the GPR model is applied to synthetic data generated in this work to investigate how the size of dataset influence the prediction of strain-rate effects. The core advantage of implementing GPR is its probabilistic framework and uncertainty estimates for predictions.

3.2. Gaussian Process Regression (GPR)

The GPR is a non-linear and non-parametric Bayesian regression model. It allows for predictions that incorporate prior knowledge through the use of kernels, while providing a measure of uncertainty for each prediction. The GPR defines a probability distribution over possible functions that could fit the data. As shown in Figure 9, this process is fundamentally based on a

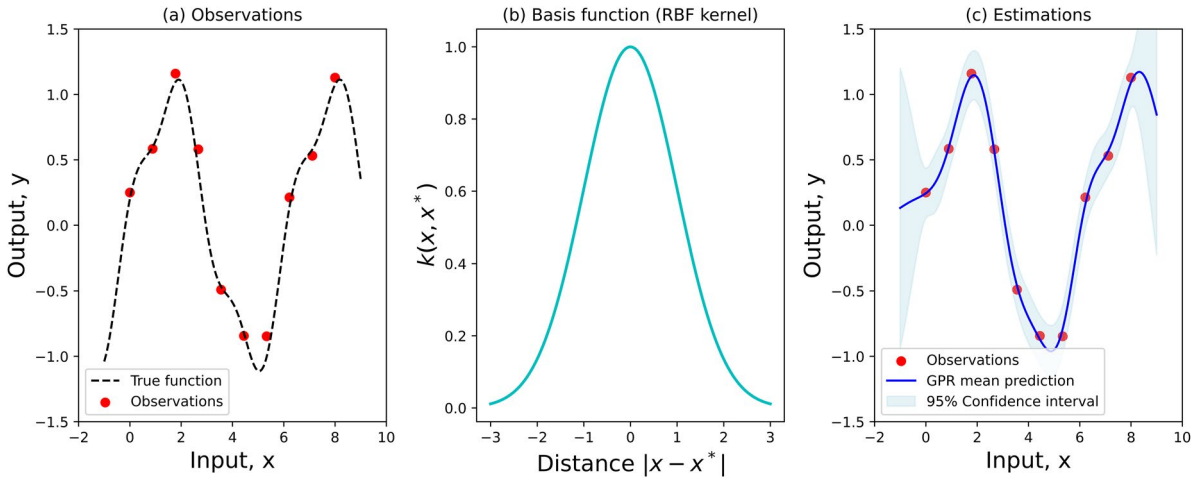

Figure 9. Basic elements of the Gaussian Process Regression (GPR): (a) an observation of an unknown function; (b) a basis function to determine the covariance; (c) an estimation by the corresponding basis functions for the prediction of the GPR model.

kernel, also known as covariance function, which describes the relationships and expected similarity between any two data points in the input space (Ariyasinghe & Herath, 2024; Deringer et al., 2021).

Given an input feature vector x in n-dimensional space ($x \in \mathbb{R}^n$), the GPR model learns an optimal mapping between the input x to the output y by defining a posterior distribution over the function. Consequently, the GPR can provide a mean value and a measure of uncertainty as confidence intervals. This characteristics makes it particularly useful for interpolation tasks in complex and high-dimensional spaces. Additionally, the kernel function governs the smoothness and generalization of the regression function. In this study, Radial Basis Function (RBF) kernel function is implemented with additional white noise covariance using scikit-learn library (Cross et al., 2024; Pedregosa et al., 2011):

$$k\left(x_i, x_j\right) = \sigma_f^2 \exp\left(-\frac{1}{2l^2}\left\|x_i - x_j\right\|^2\right) + \sigma_n^2 \delta_{ij} \qquad (9)$$

where, x_i and x_j are adjacent points. σ_f^2 is the signal variance (scaling factor), l is the length scale, and σ_n^2 is the noise variance.

3.3. Prediction with the GPR model

The baseline training dataset is prepared with strain rate as the input feature and the corresponding in-plane shear strength as the target output. Each strength value is extracted from the total 18 experimental stress-strain curves. Also, different size of datasets are prepared by supplementing the baseline dataset with varying the size of GANs-generated synthetic data to investigate the impact of the dataset size on the model performance. For each case, the respective dataset is split into training (80%) and test (20%) sets.

Following the data split, the hyperparameters for the GPR model is optimised with RBF kernel function. The Optuna library (Akiba et al., 2019) is implemented to automate the hyperparameter search. The optimisation is configured to run for 100 trials and the k-fold cross-validated RMSE is used as the objective function. The set of hyperparameters that yields the minimum cross-validated RMSE is selected as optimal set. The minimal loss $\mathcal{L}(\theta)$ is calculated as:

$$\mathcal{L}(\theta) = \sqrt{\frac{\sum_j \frac{\sum_i \left(y_{ij} - \check{y}_{ij}\right)^2}{N_j}}{k}} \qquad (10)$$

where k is the total number of fold (cross-validation), j is the index of each fold, N_j is the number of data points in j-th fold, i is the index of each data point in j-th fold, y is the true value, and $\check{y}$ is the predicted value.

The GPR model is trained with different training dataset sizes (refer to Table 4) and the resultant performance is evaluated by three evaluation metrics, the coefficient of determination (R^2), root mean squared error (RMSE), and negative log predictive density (NLPD). While R^2 indicates the mean linear trend, RMSE reflects the practical reliability of the model's prediction (i.e., how well a model fits the data) (Gupta et al., 2024). Also, the NLPD measures the predictive distribution to quantify the predictive quality of the output (i.e., more negative NLPD is better) (Y. Guan et al., 2024):

$$NLPD = -\sum_{i=1}^{N} \log p\left(y_i = (f(x_i) \mid x_i)\right) \qquad (11)$$

where, where y is the true value, $f(x)$ is the prediction, and p is the probability.

The results indicate that adding a small amount of data (300 data points) actually worsens the model's performance compared to the baseline. In contrast, adding 1800 data points leads to the outstanding predictive accuracy (R^2 and RMSE) and the excellent uncertainty calibration (NLPD). However, as more data points are added beyond this point, those metrics begin to decline. This observation demonstrates that a larger dataset is not always better. While adequate amount of synthetic data is needed to ensure high variability in training dataset, an excessive amount of synthetic data beyond this optimal point proves detrimental. Interestingly, the baseline dataset which contains only real experimental data achieves a low NLPD score. This result can be explained by the fact that the GPR model learns only the scatter of measurement (aleatoric uncertainty), which is the variation of the in-plane strength at each strain rate. Moreover, the NLPD score for the model trained with 1800 data points is similar to that of the baseline dataset, indicating that the model is closely aligned with the scatter present in the real experimental data.

As shown in Table 4, the GPR model's predictive performance shows diminishing returns beyond the dataset with 1800 samples, for which R^2 is about 0.97. To quantitatively evaluate the cause of this saturation, two-sample Kolmogorov-Smirnov (KS) tests (Lin et al., 2010; Ruiz-Gándara et al., 2025) are conducted to compare the distributions of the dataset sizes of 1800 and 3600 data points. The goodness-of-fit tests, such as the KS test, would reveal whether there are significant differences between them. The KS test calculates the distance between two independent empirical Cumulative Distribution Function (eCDF), and the KS distance is defined as follows (Lin et al., 2010):

$$D_{m,n} = sup_x \left| S_m(x) - S_n(x) \right| \qquad (12)$$

Table 4. Effect of dataset size and the summary of the model performance.

Metrics	Baseline[a] (18)	300	600	1800	3600
R^2	0.93	0.91	0.96	0.97	0.97
RMSE	0.0324	0.0642	0.0497	0.0375	0.0424
NLPD	−1.87	−1.24	−1.58	−1.88	−1.74

[a]Only real experimental data, three strength values for each of the six strain rates.

Table 5. The comparison of GAN-generated synthetic datasets with 1800 and 3600 data points using Kolmogorov–Smirnov (KS) test.

Strain-rate [s^{-1}]	KS distance	p Value	Results[a]
0.0008	0.356	0	Yes, significant difference
0.1	0.011	1	No
10	0.013	1	No
100	0.042	.62	No
200	0.016	1	No
300	0.074	.031	Yes

[a]The decision based on p value > 5% which is the usual threshold level.

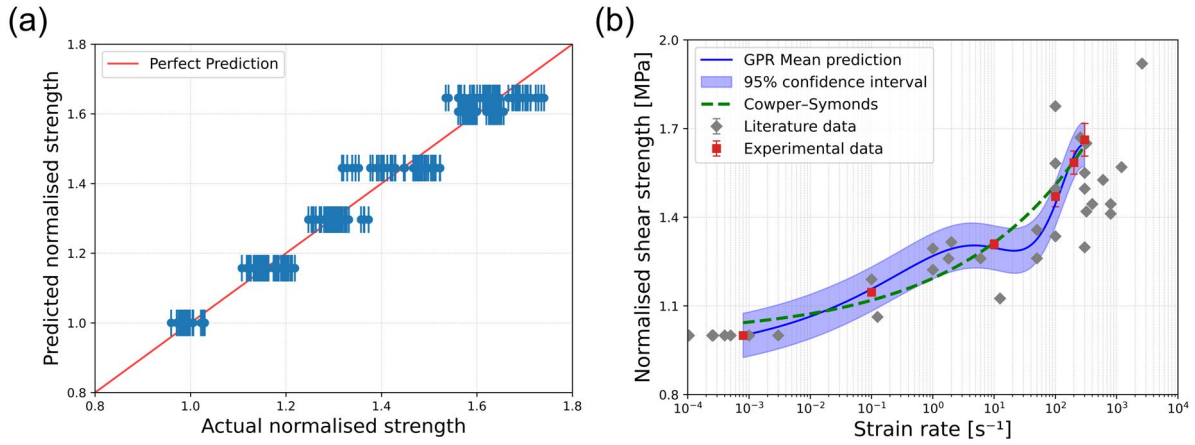

Figure 10. Gaussian Process Regression (GPR) model for predicting the strain-rate dependent in-plane shear strength of IM7/8552 composites: (a) predicted vs. actual normalized in-plane shear strength plot (red diagonal line represents the perfect prediction, $R^2 = 1$) and (b) comparative analysis of the GPR trained with 1800 data points and Cowper-Symonds model.

where, $S_m(x)$ and $S_n(x)$ are two independent eCDFs of the sample size with m and n, respectively. *sup* is the supremum (maximum) of the absolute difference over all points x.

The analysis of data distribution via the KS test reveals that the data space is largely saturated with exceptionally high p values, as shown in Table 5. This result shows that the underlying distributions of the data converge even as new data (3600) is added to the dataset, indicating that the two datasets are statistically indistinguishable.

Figure 10 shows the performance of the best GPR prediction model, which is trained on 1800 data points. Figure 10(a) compares the predicted and actual normalised in-plane shear strength, and this result indicates that the model's accuracy is high and well-calibrated (R^2 = 0.97 and RMSE = 0.0375). Also, as shown in Figure 10(b), the mean prediction from the GPR model offers a flexible best fit, enabling it to effectively learn the complex strain-rate dependent behaviour of IM7/8552 composites. In contrast, the CS model provides a simpler, and deterministic prediction that shows exponential increases in strength with increasing strain-rate. When the interpolated prediction is made, because of this rigid structure, the CS model cannot inherently capture local data variations arising from complex failure mechanisms present in FRP composites. This variation could be reflected in a shift in the failure mode as the strain-rate increases (Perry & Walley, 2022). Thus, the CS model cannot provide insight into its confidence.

A crucial finding from the GPR prediction is the non-linearity observed in the strain-rate range between 0.1 s^{-1} and 100 s^{-1}. This result deviates from the typically reported strain-rate behaviour of polymer matrix composites in literature (Klavzer et al., 2025; Thomson et al., 2025). Two possible reasons for this observation. The first one is a modelling artefact due to local variations within the dataset, and the second one is that the non-linearity is physically real, where the tested material might experience a competing phenomenon like adiabatic thermal softening at those rates, while the viscoelasticity of the matrix generally drives an increase in strength (Perry & Walley, 2022). In the meantime, the 95% confidence interval of the GPR model is wider than that of other regions. This suggests that the GPR model is uncertain in its predictions, a key advantage of probabilistic GPR models over deterministic approaches.

3.4. Hybrid approach

The GPR model presents a promising solution to be used in predicting strain-rate effects but it also has a key limitation. In the data-sparse region, especially at strain rates between 0.1 s^{-1} and 100 s^{-1}, a fluctuation is observed in predictions, indicating a lack of a solid physical basis for making confident estimates. As discussed above, the results are questionable when considering the strain-rate behaviour of the polymer matrix itself. This phenomenon could be an artifact of the GPR model attempting to align a smooth physical model with the limited available data points.

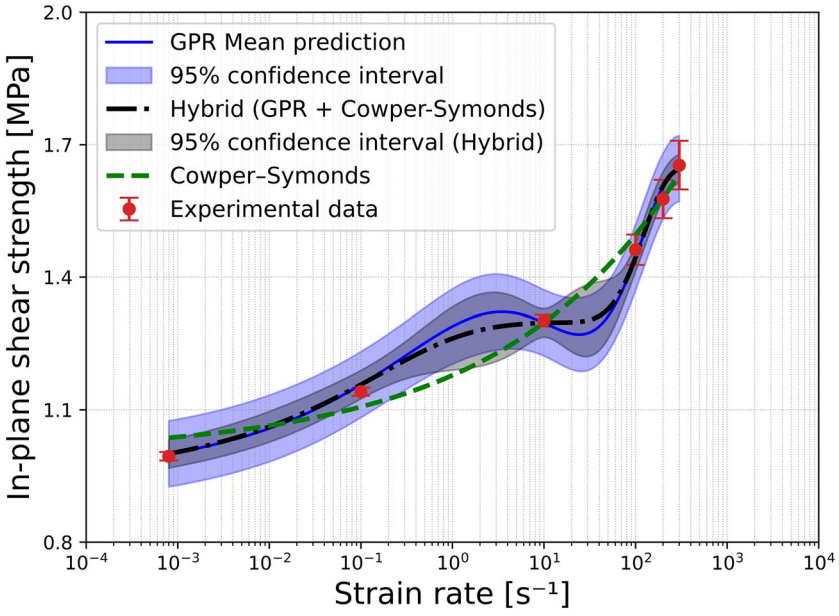

Figure 11. Comparative study of predicting the strain-rate dependent in-plane shear strength of IM7/8552 composites by using Gaussian Process Regression (GPR) model and the hybrid approach.

To address this issue, a hybrid modelling approach that integrates physical knowledge into the GRP model is proposed here by using the CS model as the mean function. The hybrid model uses the CS model to predict the main deterministic trend. The GPR model is then trained exclusively on the residuals, the error between the physical CS trend line and the actual data points. Consequently, the CS model represents a physical trend while the GPR model handles the uncertainty associated with the residuals. Figure 11 shows the GPR prediction fits from both the data-driven (blue) and hybrid (black) approaches. The comparison reveals that the hybrid model yields a narrower confidence interval, indicating a higher confidence than the pure GPR approach in the data-sparse region. This approach yields substantial improvements. In the sparse region between 0.1 and 100 s^{-1}, the average width of the 95% confidence interval is reduced by 28.9%. Also, the hybrid model reports an identical RMSE of 0.0375 on the test dataset while maintaining the same level of predictive accuracy without compromise. This reduction indicates that the physical model is effectively controlling the predictions, therefore enhancing the reliability of the hybrid model. Furthermore, the probabilistic calibration of the hybrid model obtains the NLPD of −0.59, compared to the standard GPR's −1.88 (refer to Table 4). While wider confidence bands observed in the standard GPR model naturally yield a lower NLPD, the negative value from the hybrid model confirms that it remains a well-calibrated probabilistic model. The reduction in the confidence band represents a realistic trade-off, ensuring the model does not overestimate uncertainty. Therefore, this observation highlights the true potential of the hybrid approach. Finally, future experiments should be conducted to clarify the ambiguity and experimentally confirm the material's true behaviour at strain rates in the sparse region.

4. Conclusions

This paper reports the development of a data-driven framework to address the challenge of data scarcity in the prediction of material properties, especially for FRP composites. The timeseries data augmentation method based on the GANs model is implemented, and it is found that the model is successfully employed to generate realistic material data. Additionally, an evaluation criterion for the acceptability of synthetic data is established. This criteria enable to determine synthetic data resemble to experimental data by using a statistical method, A-basis material allowables. Furthermore, to demonstrate the application of synthetic data, the GPR model is exemplary used to predict the strain-rate dependent behaviour of carbon/epoxy composites (IM7/8522).

The predicted results from the GPR model indicate that the GPR can accurately interpolate the in-plane shear strength of carbon/epoxy composites across various strain rates. High accuracy (R^2 = 0.97 and RMSE = 0.0375) is achieved using a training dataset generated through a developed data augmentation technique. Also, the study on the impact of dataset size reveals that simply increasing the dataset size does not guarantee high performance of the GPR model. It is found that the optimised dataset supplemented with 1800 synthetic data shows the highest predictive accuracy and the NLPD value of −1.88.

The application of the optimised GPR model shows that the non-linear strain-rate dependent behaviour in the range of strain-rate between 0.1 and 100 s^{-1} is unlikely to be that of the results from the CS model. This observation suggests the potential physical transitions like thermal softening, while the GPR model provides the wider confidence intervals, suggesting less confidence in the prediction. Therefore, additional experiments are required to confirm the true strain-rate dependent behaviour of carbon/epoxy composites, where the non-linearity is predicted from the GPR model. Finally, the hybrid modelling approach demonstrates how data-driven models can be integrated with physical knowledge to create more powerful and robust predictive tools. Therefore, the hybrid model of the GPR and CS models offers not only accurate predictions but also the statistical confidence that is necessary for safety-critical composite applications.

Author contributions

CRediT: **Sanghyun Yoo**: Conceptualization, Data curation, Formal analysis, Investigation, Methodology, Validation, Visualization, Writing – original draft, Writing – review & editing; **Amal Viswakumar**: Conceptualization, Data curation, Formal analysis, Investigation, Methodology, Visualization, Writing – original draft; **Mathieu Vinot**: Investigation, Methodology, Visualization, Writing – review & editing; **Nathalie Toso**: Funding acquisition, Project administration, Resources, Supervision, Writing – review & editing; **Heinz Voggenreiter**: Funding acquisition, Supervision, Writing – review & editing.

Disclosure statement

No potential conflict of interest was reported by the author(s).

Data availability statement

Data will be made available on request.

References

Akiba T, Sano S, Yanase T., et al. (Eds.). (2019). Optuna: A next-generation hyperparameter optimization framework. In *Proceedings of the 25th ACM SIGKDD International Conference on Knowledge Discovery & Data Mining* (pp. 2623-2631). https://dl.acm.org/doi/10.1145/3292500.3330701.

Alqahtani, H., Kavakli-Thorne, M., & Kumar, G. (2021). Applications of Generative Adversarial Networks (GANs): An updated review. *Archives of Computational Methods in Engineering*, *28*(2), 525–552. https://doi.org/10.1007/s11831-019-09388-y

Alzubaidi, L., Bai, J., Al-Sabaawi, A., et al. (2023). A survey on deep learning tools dealing with data scarcity: Definitions, challenges, solutions, tips, and applications. *Journal of Big Data*, *10*(1), 46. https://doi.org/10.1186/s40537-023-00727-2

Annaki, I., Rahmoune, M., & Bourhaleb, M. (2024). Overview of data augmentation techniques in time series analysis. *International Journal of Advanced Computer Science & Applications*, *15*(1). 1201-1211. https://doi.org/10.14569/IJACSA.2024.01501118

Ariyasinghe, N., & Herath, S. (2024). Machine learning techniques for predictive modelling and uncertainty quantification of the mechanical properties of woven carbon fibre composites. *Materials Today Communications*, *40*, 109732. https://doi.org/10.1016/j.mtcomm.2024.109732

ASTM D3518/D3518M-18. (2018). *Standard test method for in-plane shear response of polymer matrix composite materials by tensile test of a ±45° laminate*. ASTM International.

Bansal, A., Sharma, R., & Kathuria, M. (2022). A systematic review on data scarcity problem in deep learning: Solution and applications. *ACM Computing Surveys*, *54*(10s), 208. https://doi.org/10.1145/3502287

Chatterjee, S., Hazra, D., & Byun, Y.-C. (2025). GAN-based synthetic time-series data generation for improving prediction of demand for electric vehicles. *Expert Systems with Applications*, *264*, 125838. https://doi.org/10.1016/j.eswa.2024.125838

Cross, E. J., Rogers, T. J., Pitchforth, D. J., et al. (2024). A spectrum of physics-informed Gaussian processes for regression in engineering. *Data-Centric Engineering*, *5*, e8. https://doi.org/10.1017/dce.2024.2

Cui, H., Thomson, D., Pellegrino, A., et al. (2016). Effect of strain rate and fibre rotation on the in-plane shear response of ±45° laminates in tension and compression tests. *Composites Science and Technology*, *135*, 106–115. https://doi.org/10.1016/j.compscitech.2016.09.016

Cumbo, R., Baroni, A., Ricciardi, A., et al. (2022). Design allowables of composite laminates: A review. *Journal of Composite Materials*, *56*(23), 3617–3634. https://doi.org/10.1177/00219983221117216

Daniel, I. M., Daniel, S. M., & Fenner, J. S. (2018). A new yield and failure theory for composite materials under static and dynamic loading. *International Journal of Solids and Structures*, *148-149*, 79–93. https://doi.org/10.1016/j.ijsolstr.2017.08.036

Demir, S., Mincev, K., Kok, K., et al. (2021). Data augmentation for time series regression: Applying transformations, autoencoders and adversarial networks to electricity price forecasting. *Applied Energy*, *304*, 117695. https://doi.org/10.1016/j.apenergy.2021.117695

Deringer, V. L., Bartók, A. P., Bernstein, N., et al. (2021). Gaussian Process Regression for materials and molecules. *Chemical Reviews*, *121*(16), 10073–10141. https://doi.org/10.1021/acs.chemrev.1c00022

Dev, B., Rahman, M. A., Islam, M. J., et al. (2024). Properties prediction of composites based on machine learning models: A focus on statistical index approaches. *Materials Today Communications*, *38*, 107659. https://doi.org/10.1016/j.mtcomm.2023.107659

Dornheim, J., Morand, L., Nallani, H. J., et al. (2024). Neural networks for constitutive modeling: From universal function approximators to advanced models and the integration of physics. *Archives of Computational Methods in Engineering*, *31*(2), 1097–1127. https://doi.org/10.1007/s11831-023-10009-y

Freed, Y., Zobeiry, N., & Salviato, M. (2022). Development of aviation industry-oriented methodology for failure predictions of brittle bonded joints using probabilistic machine learning. *Composite Structures*, *297*, 115979. https://doi.org/10.1016/j.compstruct.2022.115979

Furtado, C., Pereira, L. F., Tavares, R. P., et al. (2021). A methodology to generate design allowables of composite laminates using machine learning. *International Journal of Solids and Structures*, *233*, 111095. https://doi.org/10.1016/j.ijsolstr.2021.111095

Ge, J., Zhang, J., Xu, M., et al. (2025). Data-driven CFRP machining performance prediction and optimization: Advances, challenges and future prospects. *Thin-Walled Structures*, *216*, 113721. https://doi.org/10.1016/j.tws.2025.113721

Gilat, A., Goldberg, R. K., & Roberts, G. D. (2002). Experimental study of strain-rate-dependent behavior of carbon/epoxy composite. *Composites Science and Technology*, *62*(10–11), 1469–1476. https://doi.org/10.1016/S0266-3538(02)00100-8

Goodfellow, I., Pouget-Abadie, J., Mirza, M., et al. (2014). Generative adversarial nets. *Advances in Neural Information Processing Systems (NIPS 2014)*, *27*, 2672–2680.

Guan, S., & Loew, M. (Eds.). (2019, October 15–17). *Evaluation of Generative Adversarial Network performance based on direct analysis of generated images* [Paper presentation]. Washington, USA: 2019 IEEE Applied Imagery Pattern Recognition Workshop (AIPR). https://doi.org/10.1109/AIPR47015.2019.9174595

Guan, Y., He, S., Ren, S., et al. (2024). Mixture Gaussian process model with Gaussian mixture distribution for big data. *Chemometrics and Intelligent Laboratory Systems*, *253*, 105201. https://doi.org/10.1016/j.chemolab.2024.105201

Gupta, M. K., Korkmaz, M. E., Karolczuk, A., et al. (2024). A study on friction induced tribological characteristics of steel 316 L against 100 cr6 alloy under different lubricating conditions with machine learning model. *Tribology International*, *195*, 109599. https://doi.org/10.1016/j.triboint.2024.109599

Hakami, A. (2024). Strategies for overcoming data scarcity, imbalance, and feature selection challenges in machine learning models for predictive maintenance. *Scientific Reports*, *14*(1), 9645. https://doi.org/10.1038/s41598-024-59958-9

Heusel, M., Ramsauer, H., Unterthiner, T., et al. (2017). Gans trained by a two time-scale update rule converge to a local Nash equilibrium. *Advances in Neural Information Processing Systems*, *30*, 6626–6637.

Ho, J., Jain, A., & Abbeel, P. (2020). Denoising diffusion probabilistic models. *Advances in Neural Information Processing Systems*, *33*, 6840–6851.

Hsiao, H. M., Daniel, I. M., & Cordes, R. D. (1999). Strain rate effects on the transverse compressive and shear behavior of unidirectional composites. *Journal of Composite Materials*, *33*(17), 1620–1642. https://doi.org/10.1177/002199839903301703

Huang, J. S., Liew, J. X., & Liew, K. M. (2021). Data-driven machine learning approach for exploring and assessing mechanical properties of carbon nanotube-reinforced cement composites. *Composite Structures*, *267*, 113917. https://doi.org/10.1016/j.compstruct.2021.113917

Iglesias, G., Talavera, E., González-Prieto, Á., et al. (2023). Data Augmentation techniques in time series domain: A survey and taxonomy. *Neural Computing and Applications*, *35*(14), 10123–10145. https://doi.org/10.1007/s00521-023-08459-3

Iwana, B. K., & Uchida, S. (2021). An empirical survey of data augmentation for time series classification with neural networks. *PLoS One*, *16*(7), e0254841. https://doi.org/10.1371/journal.pone.0254841

Jain, S., Seth, G., Paruthi, A., et al. (2022). Synthetic data augmentation for surface defect detection and classification using deep learning. *Journal of Intelligent Manufacturing*, *33*(4), 1007–1020. https://doi.org/10.1007/s10845-020-01710-x

Karamov, R., Akhatov, I., & Sergeichev, I. V. (2022). Prediction of fracture toughness of pultruded composites based on supervised machine learning. *Polymers*, *14*(17), 3619. https://doi.org/10.3390/polym14173619

Kibrete, F., Trzepieciński, T., Gebremedhen, H. S., et al. (2023). Artificial Intelligence in predicting mechanical properties of composite materials. *Journal of Composites Science*, *7*(9), 364. https://doi.org/10.3390/jcs7090364

Kingma, D. P., & Welling, M. (2019). An introduction to variational autoencoders. *Foundations and Trends® in Machine Learning*, *12*(4), 307–392. https://doi.org/10.1561/2200000056

Klavzer, N., Chevalier, J., Breite, C., et al. (2025). Master trends in the elasto-viscoplastic behaviour of highly cross-linked epoxy resins. *Mechanics of Time-Dependent Materials*, *29*(3), 68. https://doi.org/10.1007/s11043-025-09804-w

Koerber, H., Kuhn, P., Ploeckl, M., et al. (2018). Experimental characterization and constitutive modeling of the non-linear stress–strain behavior of unidirectional carbon–epoxy under high strain rate loading [journal article]. *Advanced Modeling and Simulation in Engineering Sciences*, *5*(1), 17. https://doi.org/10.1186/s40323-018-0111-x

Koerber, H., Xavier, J., & Camanho, P. P. (2010). High strain rate characterisation of unidirectional carbon-epoxy IM7-8552 in transverse compression and in-plane shear using digital image correlation. *Mechanics of Materials*, *42*(11), 1004–1019. https://doi.org/10.1016/j.mechmat.2010.09.003

Ledford, N., Imbert, M., & May, M. (2021). High-rate in-plane shear testing of IM7/8552 using the split Hopkinson tension bar. *AIAA Journal*, *59*(10), 4257–4263. https://doi.org/10.2514/1.J060269

Liaw, R., Liang, E., Nishihara, R., et al. (2018). Tune: A research platform for distributed model selection and training. arXiv preprint arXiv:1807.05118. https://doi.org/10.48550/arXiv.1807.05118

Lienhard, J., & Böhme, W. (2015). Characterisation of resin transfer moulded composite laminates under high rate tension, compression and shear loading. *Engineering Fracture Mechanics*, *149*, 338–350. https://doi.org/10.1016/j.engfracmech.2015.07.012

Lin, P.-C., Wu, B., & Watada, J. (2010). Kolmogorov-Smirnov two sample test with continuous fuzzy data. In V.-N. Huynh, Y. Nakamori, J. Lawry, et al. (Eds.), *Integrated uncertainty management and applications* (pp. 175–186). Springer. https://doi.org/10.1007/978-3-642-11960-6_17

Liu, L.-M., Ren, X.-Y., Zhang, F., et al. (2023). Dual-dimension time-GGAN data augmentation method for improving the performance of deep learning models for PV power forecasting. *Energy Reports*, *9*, 6419–6433. https://doi.org/10.1016/j.egyr.2023.05.226

Liu, M., Li, H., Zhou, H., et al. (2024). Development of machine learning methods for mechanical problems associated with fibre composite materials: A review. *Composites Communications*, *49*, 101988. https://doi.org/10.1016/j.coco.2024.101988

Liu, Q., & Wu, D. (2024). Machine learning and feature representation approaches to predict stress-strain curves of additively manufactured metamaterials with varying structure and process parameters. *Materials & Design*, *241*, 112932. https://doi.org/10.1016/j.matdes.2024.112932

Liu, X., Qin, J., Zhao, K., et al. (2023). Design optimization of laminated composite structures using artificial neural network and genetic algorithm. *Composite Structures*, *305*, 116500. https://doi.org/10.1016/j.compstruct.2022.116500

Liu, X., Tian, S., Tao, F., et al. (2021). A review of artificial neural networks in the constitutive modeling of composite materials. *Composites Part B Engineering*, *224*, 109152. https://doi.org/10.1016/j.compositesb.2021.109152

Luleci, F., & Catbas, F. N. (2023). A brief introductory review to deep generative models for civil structural health monitoring. *AI in Civil Engineering*, *2*(1), 9. https://doi.org/10.1007/s43503-023-00017-z

Malashin, I. P., Martysyuk, D., Nelyub, V., et al. (2025). Deep learning for property prediction of natural fiber polymer composites. *Scientific Reports*, *15*(1), 27837. https://doi.org/10.1038/s41598-025-10841-1

Melching, D., Schultheis, E., & Breitbarth, E. (2023). Generating artificial displacement data of cracked specimen using physics-guided adversarial networks. *Machine Learning: Science and Technology*, *4*(4), 045063.

Nikitin, A., Iannucci, L., & Kaski, S. (2024). TSGM: A flexible framework for generative modeling of synthetic time series. *Advances in Neural Information Processing Systems*, *37*, 129042–129061.

Pandya, K. S., Roth, C. C., & Mohr, D. (2020). Strain rate and temperature dependent fracture of aluminum alloy 7075: Experiments and neural network modeling. *International Journal of Plasticity*, *135*, 102788. https://doi.org/10.1016/j.ijplas.2020.102788

Paszke, A., Gross, S., Massa, F., et al. (2019). Pytorch: An imperative style, high-performance deep learning library. *Advances in Neural Information Processing Systems*, *32*, 8026-8037.

Pedregosa, F., Varoquaux, G., Gramfort, A., et al. (2011). Scikit-learn: Machine learning in Python. *Journal of Machine Learning Research*. *12*, 2825–2830.

Perry, J. I., & Walley, S. M. (2022). Measuring the effect of strain rate on deformation and damage in fibre-reinforced composites: A review. *Journal of Dynamic Behavior of Materials*, *8*(2), 178–213. https://doi.org/10.1007/s40870-022-00331-0

Qu, H., Hu, T., Qu, J., et al. (2025). A machine learning model based on GAN-ANN data augmentation for predicting the bond strength of FRP-reinforced concrete under high-temperature conditions. *Composite Structures*, *369*, 119321. https://doi.org/10.1016/j.compstruct.2025.119321

Reiner, J., Vaziri, R., & Zobeiry, N. (2021). Machine learning assisted characterisation and simulation of compressive damage in composite laminates. *Composite Structures*, *273*, 114290. https://doi.org/10.1016/j.compstruct.2021.114290

Rouf, K., Worswick, M., & Montesano, J. (2024). Effect of strain rate on the in-plane orthotropic constitutive response and failure behaviour of a unidirectional non-crimp fabric composite. *Composites Part A Applied Science and Manufacturing*, *181*, 108166. https://doi.org/10.1016/j.compositesa.2024.108166

Ruiz-Gándara, A., Casales-García, V., & González-Abril, L. (2025). Artificial generation of survey data on the expected bitterness of beer. *Expert Systems with Applications*, *275*, 126950. https://doi.org/10.1016/j.eswa.2025.126950

SAE International. (2012). Composite materials handbook. In *Polymer matrix composites guideline for characterization of structural materials* (131-159). SAE International.

Sakaridis, E., Karathanasopoulos, N., & Mohr, D. (2022). Machine-learning based prediction of crash response of tubular structures. *International Journal of Impact Engineering*, *166*, 104240. https://doi.org/10.1016/j.ijimpeng.2022.104240

Shah, V., Zadourian, S., Yang, C., et al. (2022). Data-driven approach for the prediction of mechanical properties of carbon fiber reinforced composites. *Materials Advances*, *3*(19), 7319–7327. https://doi.org/10.1039/D2MA00698G

Snoek, J., Larochelle, H., & Adams, R. P. (2012). Practical Bayesian optimization of machine learning algorithms. *Advances in Neural Information Processing Systems (NIPS 2012)*, *25*, 2951–2959.

Sorour, S. S., Saleh, C. A., & Shazly, M. (2024). A review on machine learning implementation for predicting and optimizing the mechanical behaviour of laminated fiber-reinforced polymer composites. *Heliyon*, *10*(13), e33681. https://doi.org/10.1016/j.heliyon.2024.e33681

Su, N., Guo, S., Shi, C., et al. (2024). Predictions of mechanical properties of fiber reinforced concrete using ensemble learning models. *Journal of Building Engineering*, *98*, 110990. https://doi.org/10.1016/j.jobe.2024.110990

Taniguchi, N., Nishiwaki, T., & Kawada, H. (2007). Tensile strength of unidirectional CFRP laminate under high strain rate. *Advanced Composite Materials*, *16*(2), 167–180. https://doi.org/10.1163/156855107780918937

Taniguchi, N., Nishiwaki, T., & Kawada, H. (2008). Experimental characterization of dynamic tensile strength in unidirectional carbon/epoxy composites. *Advanced Composite Materials*, *17*(2), 139–156. https://doi.org/10.1163/156855108X314779

Thomson, D. M., Cui, H., Erice, B., et al. (2017). Experimental and numerical study of strain-rate effects on the IFF fracture angle using a new efficient implementation of Puck's criterion. *Composite Structures*, *181*, 325–335. https://doi.org/10.1016/j.compstruct.2017.08.084

Thomson, D., Ploeckl, M., Hoffmann, J., et al. (2025). A review of the effect of loading rate on the mechanical properties of unidirectional carbon fibre reinforced polymer composites. *Composites Part A Applied Science and Manufacturing*, *193*, 108773. https://doi.org/10.1016/j.compositesa.2025.108773

Tomblin, J. S., Ng, Y. C., & Raju, K. S. (2003). *Material qualification and equivalency for polymer matrix composite material systems: Updated procedure*. Office of Aviation Research, Federal Aviation Administration.

Turowski, M., Heidrich, B., Weingärtner, L., et al. (2024). Generating synthetic energy time series: A review. *Renewable and Sustainable Energy Reviews*, *206*, 114842. https://doi.org/10.1016/j.rser.2024.114842

Vincent, A. M., & Jidesh, P. (2023). An improved hyperparameter optimization framework for AutoML systems using evolutionary algorithms. *Scientific Reports*, *13*(1), 4737. https://doi.org/10.1038/s41598-023-32027-3

Wang, X., Jin, Y., Schmitt, S., et al. (2023). Recent advances in Bayesian optimization. *ACM Computing Surveys*, *55*(13s), 1-36. https://doi.org/10.1145/3582078

Wen Q, Sun L, Yang F., et al. (Eds.). (2021). Time series data augmentation for deep learning: A survey. In *Proceedings of the Thirtieth International Joint Conference on Artificial Intelligence (IJCAI-21)*. International Joint Conferences on Artificial Intelligence (pp. 4653-4660). https://doi.org/10.24963/ijcai.2021/631.

Yang, H., Xiang, Z., Li, X., et al. (2025). An improved GAN-based data augmentation model for addressing data scarcity in SRMs. *Measurement Science and Technology*, *36*(2), 026129. https://doi.org/10.1088/1361-6501/ada570

Yang, L., & Shami, A. (2020). On hyperparameter optimization of machine learning algorithms: Theory and practice. *Neurocomputing*, *415*, 295–316. https://doi.org/10.1016/j.neucom.2020.07.061

Yoo, S., Dalli, D., Catalanotti, G., et al. (2022). Dynamic intralaminar fracture toughness characterisation of unidirectional carbon fibre-reinforced polymer composites using a high-speed servo-hydraulic test set-up. *Composite Structures*, *295*, 115838. https://doi.org/10.1016/j.compstruct.2022.115838

Zhang, C., Li, Y., Jiang, B., et al. (2022). Mechanical properties prediction of composite laminate with FEA and machine learning coupled method. *Composite Structures*, *299*, 116086. https://doi.org/10.1016/j.compstruct.2022.116086

Zhou, S., Sun, Z., Li, W., et al. (2025). A hybrid machine learning framework with GAN-based data augmentation for predicting strain properties of fiber-reinforced repair mortar. *Journal of Building Engineering*, *114*, 114140. https://doi.org/10.1016/j.jobe.2025.114140